



# A warming adjustment method for CORDEX RCM simulations

Stefanie Börsig<sup>1</sup>, Dominik L. Schumacher<sup>1</sup>, and Sonia I. Seneviratne<sup>1</sup>

<sup>1</sup>Institute for Atmospheric and Climate Science, Department of Environmental Systems Science, ETH Zurich, Zürich, Switzerland

**Correspondence:** Stefanie Börsig (stefanie.boersig@env.ethz.ch)

## Abstract.

Regional climate model (RCM) projections provide high-resolution information essential for climate impact assessments and adaptation planning. Currently available Coordinated Regional Climate Downscaling Experiment (CORDEX) simulations, driven by CMIP5 global models, exhibit considerably weaker European warming throughout the 21st century compared to the latest Coupled Model Intercomparison Phase 6 (CMIP6) models. This discrepancy arises from multiple factors: RCMs tend to underestimate warming compared to their driving models in part due to the use of aerosol climatologies, while CMIP6 models themselves exhibit higher climate sensitivity than their CMIP5 predecessors. Here, we present a method to adjust existing CORDEX simulations toward the large-scale warming simulated by CMIP6 models while preserving fine-scale spatial structure and physical coherence. The method operates by reassembling complete annual fields from the original simulations according to smoothed temperature trajectories, maintaining temporal monotonicity without requiring interpolation. We demonstrate its application to both temperature and precipitation, including mean conditions and extremes over Europe, though the approach is applicable to any regional domain and warming-sensitive climate variable. As an extension, the method can be applied sequentially to establish consistency from prescribed global warming levels through CMIP6 regional patterns to high-resolution RCM projections. This bridges the temporal gap between regional and global model development cycles, making existing high-resolution climate information compatible with both updated model generations and specific warming targets.

# 1 Introduction

Robust regional climate projections are essential for impact assessments, adaptation strategies, and climate services. Although global climate model (GCM) experiments compiled under the Coupled Model Intercomparison Phase 6 (CMIP6) provide the foundation for understanding climate trajectories (Eyring et al., 2016), their coarse spatial resolution limits direct usability for regional-to-local-scale studies, particularly in the presence of complex orography. The Coordinated Regional Climate Downscaling Experiment (CORDEX) initiative was established to address this gap by providing a coordinated framework for regional downscaling of global climate simulations (Giorgi and Gutowski Jr., 2015; Gutowski Jr. et al., 2016). Simulations contributing to CORDEX provide high-resolution regional climate model (RCM) information with continuous, long-term coverage needed for climate projections, and are thus widely used in both scientific assessments and policy contexts.

https://doi.org/10.5194/egusphere-2025-4968 Preprint. Discussion started: 10 November 2025

© Author(s) 2025. CC BY 4.0 License.





Nevertheless, challenges remain in reconciling information across different generations of climate projections. EURO-CORDEX simulations tend to underestimate historical and projected warming in Europe compared to their driving CMIP5 models (Schumacher et al., 2024). Most currently available RCM experiments employ aerosol climatologies rather than transient forcing, failing to capture the strong observed brightening owing to reduced anthropogenic aerosol loads since the 1980s (Wild et al., 2005, 2021) and its associated warming signal (e.g., Bartók et al., 2017; Boé et al., 2020; Persad et al., 2023; Schumacher et al., 2024). Consequently, the regional response to global warming is systematically underestimated in existing high-resolution region projections.

Meanwhile, CMIP6 models show a substantially wider range of equilibrium climate sensitivity and a modestly wider range of transient climate response compared to CMIP5 (Meehl et al., 2020). Approximately one-third of CMIP6 models exceed the IPCC Fifth Assessment Report's likely range, with this increased equilibrium climate sensitivity linked primarily to stronger positive cloud feedbacks from extratropical low cloud changes (Zelinka et al., 2020). This elevated sensitivity translates to stronger warming trajectories that may be implausible given observational constraints of past warming (Tokarska et al., 2020; Lee et al., 2021). However, regional patterns of warming per degree of global change remain broadly consistent across CMIP5 and CMIP6 cycles (Seneviratne and Hauser, 2020; Wehner, 2020; Li et al., 2021; Seneviratne et al., 2021).

Taken together, RCMs thus tend to simulate less warming than CMIP5 GCMs, while CMIP6 GCMs on average project more, creating an inconsistency between existing high-resolution regional simulations and the trajectories implied by the newer global model generation. This misalignment is problematic in the time domain: RCM projections driven by CMIP5 models reach regional warming levels at different times than their global CMIP6 counterparts, undermining the temporal consistency critical for impact assessments and adaptation planning (Diez-Sierra et al., 2023).

We present a warming-adjustment method designed to bridge this gap. Conceptually, our approach resembles earlier work in which decadal slices of GCM output were recombined, or 'stitched' together, to follow prescribed global warming trajectories (Tebaldi et al., 2022). However, our method tackles a different problem: rather than emulating GCM-like output for predefined warming scenarios, it harmonizes existing high-resolution regional climate projections with updated global and regional warming constraints, while preserving their fine-scale spatial detail and physical coherence. This is achieved by performing the adjustment on annual mean warming and reassembling existing data without interpolation, thereby enabling cross-variable consistency. In doing so, we provide a coherent framework that enables existing high-resolution RCM simulations to become compatible with observationally constrained global warming trajectories on the one hand, and with the regional warming responses simulated by the latest CMIP6 global climate models on the other. This harmonization makes full use of the resolution advantage inherent to regional climate model simulations while ensuring these projections remain scientifically consistent with both observational constraints and the most current understanding of climate system behavior, thereby enhancing the robustness and utility of high-resolution climate information for impact assessments and adaptation planning.





## 2 Method

70

#### 2.1 Data sources

We demonstrate the warming adjustment method using European climate projections as a test case, comparing EURO-CORDEX simulations (Jacob et al., 2014) with output from CMIP6 global climate models (Eyring et al., 2016). These CORDEX simulations were produced with CMIP5 GCM–RCM modeling chains, and we employ EUR-11 simulations on the finest grid available for the European domain at 0.11 degrees horizontal resolution (shown in Table 1). CMIP6 simulations are processed in their native horizontal resolution to calculate regional averages and regridded to a  $1^{\circ} \times 1^{\circ}$  grid for spatial comparisons to RCM projections. We showcase the method and perform an analysis for a subset of CMIP6 models designated to provide boundary conditions for the next generation of EURO-CORDEX regional downscaling experiments (listed in Table 2; Sobolowski et al., 2023).

These CMIP6 models exhibit stronger warming trajectories than the CMIP5-driven EURO-CORDEX simulations currently available; under their respective high-emission scenarios (SSP5-8.5 and RCP8.5) and by mid-century, the CMIP6 models project markedly higher temperature increases across nonmaritime Western Europe (Fig. 1a). The mean warming across these two model ensembles further diverges in time, illustrated here as a regional average for Western Europe (Fig. 1b). This domain corresponds to the western half of the SREX region West-Central Europe, one of the IPCC climate reference regions (Iturbide et al., 2020), and is referred to as "WWCE" onwards. WWCE is used here to both establish consistent large-scale warming between RCM and GCM simulations and present results, but the approach could be applied to any other part of the world.

# 2.2 Warming adjustment algorithm

The warming adjustment operates on spatially averaged annual mean temperatures from simulation pairs over a specified domain to capture large-scale temperature changes. Here, we apply the method to align RCM simulations with their driving GCMs over WWCE. Since the goal is to match the warming evolution rather than, for example, the interannual variability of the GCM, both input time series for an RCM-GCM pair are first smoothed using a locally weighted regression (step 1 in Fig. 1c), using the recommended window size of 42 years by Scherrer et al. (2024). This choice is motivated by the fact that using a locally weighted regression does not, unlike conventional moving averages, result in a loss of data.

Then, for each requested output year, the GCM target temperature is taken, the closest matching RCM temperature is identified, and the associated year is recorded (step 2 in Fig. 1c). This yields a mapping of output (or GCM) to input (or RCM) years, and the latter typically feature temporal discontinuities and/or duplicated years (see markers in Fig. 1c, step 3). When RCM years repeat at the beginning or end of the mapping, this indicates the RCM temperature range has been exhausted (i.e., no warmer or cooler analog years exist). Such edge repeats are hence filtered (cf. grey and black dots in Fig. 1c step 3). Next, to diminish the influence of irregularities in the year-to-year mapping while preserving consistency with respect to the GCM warming trajectory, the filtered RCM–GCM year mapping is linearized in 20-year segments. This segment length was chosen empirically as a trade-off between maintaining accuracy in the temperature match and minimizing the extent of data manipulations. A linear regression is performed on the matched years, beginning with the first 20 mapped RCM–GCM years. The first segment begins

© Author(s) 2025. CC BY 4.0 License.



100



Table 1. Overview of CORDEX EUR-11 simulations used in this study, showing the unique regional climate models (RCMs), their driving CMIP5 global climate models (GCMs), and the corresponding ensemble members.

RCM	Driving GCM	Ensemble member	RCM	Driving GCM	Ensemble member
CLMcom-CCLM4-8-17	CCCma-CanESM2	rlilp1	GERICS-REMO2015	NCC-NorESM1-M	rlilp1
CLMcom-CCLM4-8-17	CNRM-CERFACS-CNRM-CM5	rlilp1	ICTP-RegCM4-6	CNRM-CERFACS-CNRM-CM5	rli1p1
CLMcom-CCLM4-8-17	ICHEC-EC-EARTH	r12i1p1	ICTP-RegCM4-6	ICHEC-EC-EARTH	r12i1p1
CLMcom-CCLM4-8-17	MIROC-MIROC5	rli1p1	ICTP-RegCM4-6	MOHC-HadGEM2-ES	rlilp1
CLMcom-CCLM4-8-17	MOHC-HadGEM2-ES	rli1p1	ICTP-RegCM4-6	MPI-M-MPI-ESM-LR	rli1p1
CLMcom-CCLM4-8-17	MPI-M-MPI-ESM-LR	rlilp1	ICTP-RegCM4-6	NCC-NorESM1-M	rlilp1
CLMcom-ETH-COSMO-crCLIM-v1-1	CNRM-CERFACS-CNRM-CM5	rlilp1	IPSL-INERIS-WRF331F	IPSL-IPSL-CM5A-MR	rli1p1
CLMcom-ETH-COSMO-crCLIM-v1-1	ICHEC-EC-EARTH	rlilp1	KNMI-RACMO22E	CNRM-CERFACS-CNRM-CM5	rli1p1
CLMcom-ETH-COSMO-crCLIM-v1-1	MOHC-HadGEM2-ES	rlilp1	KNMI-RACMO22E	ICHEC-EC-EARTH	rlilpl
CLMcom-ETH-COSMO-crCLIM-v1-1	MPI-M-MPI-ESM-LR	rlilp1	KNMI-RACMO22E	IPSL-IPSL-CM5A-MR	rlilpl
CLMcom-ETH-COSMO-crCLIM-v1-1	NCC-NorESM1-M	rlilp1	KNMI-RACMO22E	MOHC-HadGEM2-ES	rlilpl
CNRM-ALADIN53	CNRM-CERFACS-CNRM-CM5	rlilp1	KNMI-RACMO22E	MPI-M-MPI-ESM-LR	rlilpl
CNRM-ALADIN63	CNRM-CERFACS-CNRM-CM5	rlilp1	KNMI-RACMO22E	NCC-NorESM1-M	rlilpl
CNRM-ALADIN63	MOHC-HadGEM2-ES	rlilp1	MOHC-HadREM3-GA7-05	CNRM-CERFACS-CNRM-CM5	rlilpl
CNRM-ALADIN63	MPI-M-MPI-ESM-LR	rlilp1	MOHC-HadREM3-GA7-05	ICHEC-EC-EARTH	r12i1p1
CNRM-ALADIN63	NCC-NorESM1-M	rli1p1	MOHC-HadREM3-GA7-05	MPI-M-MPI-ESM-LR	rli1p1
DMI-HIRHAM5	ICHEC-EC-EARTH	rlilp1	MOHC-HadREM3-GA7-05	NCC-NorESM1-M	rlilpl
DMI-HIRHAM5	IPSL-IPSL-CM5A-MR	rlilp1	MPI-CSC-REMO2009	MPI-M-MPI-ESM-LR	rli1p1
DMI-HIRHAM5	MOHC-HadGEM2-ES	rli1p1	RMIB-UGent-ALARO-0	CNRM-CERFACS-CNRM-CM5	rli1p1
DMI-HIRHAM5	MPI-M-MPI-ESM-LR	rlilp1	SMHI-RCA4	CNRM-CERFACS-CNRM-CM5	rlilpl
DMI-HIRHAM5	NCC-NorESM1-M	rlilp1	SMHI-RCA4	ICHEC-EC-EARTH	rli1p1
GERICS-REMO2015	CCCma-CanESM2	rlilp1	SMHI-RCA4	IPSL-IPSL-CM5A-MR	rlilpl
GERICS-REMO2015	CNRM-CERFACS-CNRM-CM5	rlilp1	SMHI-RCA4	MOHC-HadGEM2-ES	rli1p1
GERICS-REMO2015	ICHEC-EC-EARTH	r12i1p1	SMHI-RCA4	MPI-M-MPI-ESM-LR	rli1p1
GERICS-REMO2015	IPSL-IPSL-CM5A-MR	rlilp1	SMHI-RCA4	NCC-NorESM1-M	rli1p1
GERICS-REMO2015	MIROC-MIROC5	rlilp1	UHOH-WRF361H	ICHEC-EC-EARTH	rli1p1
GERICS-REMO2015	MOHC-HadGEM2-ES	rlilp1	UHOH-WRF361H	MIROC-MIROC5	r1i1p1
GERICS-REMO2015	MPI-M-MPI-ESM-LR	r3i1p1	UHOH-WRF361H	MOHC-HadGEM2-ES	rlilpl

in 1991, corresponding to the start of the current WMO reference period (1991-2020) and our analysis timeframe. Segment endpoints are enforced to connect seamlessly, ensuring temporal continuity across all output years (green line in Fig. 1c, step 3).

The linearized mapping determines which RCM years are selected for each target GCM year. When the target warming evolves more quickly (slowly) than in the original RCM simulation, the latter is effectively squeezed (stretched) by removing (duplicating) a subset of RCM years. The full RCM dataset is then reassembled according to this mapping, yielding consistent large-scale warming evolution with respect to the target GCM (step 4 in Fig. 1c).

As a further constraint to regularize the mapping and limit the number of interventions with respect to the original RCM data, a minimum slope of 0.75 is enforced in the RCM-to-GCM mapping. This ensures that RCM time progresses as GCM time advances: for every 4 GCM years, at least 3 distinct RCM years must be used (i.e., at most one RCM year can be duplicated per 4-year window). Finally, when consecutive RCM duplicate years would otherwise occur, they are iteratively resolved by

© Author(s) 2025. CC BY 4.0 License.





**Table 2. Overview of the CMIP6 GCMs used in this study.** The CMIP6 GCMs are selected for boundary conditions in the next-generation EURO-CORDEX downscaling experiments (Sobolowski et al., 2023). CMIP6 models are listed with their corresponding runs, modelling centers, and institutions/contributions.

Model Name	Run	Modelling Center	Institution / Contribution	
MPI-ESM1-2-LR	rli1p1f1	MPI-M	Max Planck Institute for Meteorology, Germany	
NorESM2-MM	rli1p1f1	NCC	Norwegian Climate Centre, Norway	
MIROC6	rli1p1f1	MIROC	University of Tokyo, Atmosphere and Ocean Research Institute, Japan	
MPI-ESM1-2-HR	rli1p1f1	MPI-M	Max Planck Institute for Meteorology, Germany	
CNRM-ESM2-1	r1i1p1f2	CNRM-CERFACS	Centre National de Recherches Météorologiques, France	
CESM2	rli1p1f1	NCAR	National Center for Atmospheric Research, USA	
CMCC-CM2-SR5	rli1p1f1	CMCC	Centro Euro-Mediterraneo sui Cambiamenti Climatici, Italy	
IPSL-CM6A-LR	rli1p1f1	IPSL	Institut Pierre-Simon Laplace, France	
EC-Earth3-Veg	rli1p1f1	EC-Earth Consortium	European Consortium for Earth-System Modelling	
UKESM1-0-LL	rli1p1f2	UK Met Office	Met Office Hadley Centre, United Kingdom	

swapping latter duplicates with subsequent non-duplicate values until no consecutive duplicates remain; [2010, 2011, 2011, 2012, 2013, 2014, 2014] becomes [2010, 2011, 2012, 2011, 2012, 2013, 2014]. This preserves temporal progression while avoiding sampling the same year consecutively.

The warming-adjustment method is designed to harmonize large-scale temperature evolution across model generations and is most appropriate for climate variables whose long-term changes are primarily temperature-driven. Once a year-to-year mapping is established based on temperature matching, it can be transferred to other variables such as precipitation, wind, and temperature extremes. However, several considerations and limitations should be noted.

First, caution is warranted for variables with temporal memory effects, such as soil moisture or snow cover. Since the adjustment may duplicate or skip years, variables that depend on antecedent conditions may exhibit discontinuities, especially at sub-monthly timescales.

Second, while the method compensates for underestimated warming in CORDEX simulations with fixed aerosol representations by effectively accelerating the warming trajectory through selective year sampling, it cannot account for all physical consequences of declining aerosol emissions. Specifically, the reduction in anthropogenic aerosols since the 1980s has led not only to warming but also to increased surface shortwave radiation due to clearer atmospheric conditions (Wild et al., 2005, 2021). Since the adjustment operates by reassembling existing simulation years rather than modifying the underlying physics, the radiation fields in the adjusted data remain unchanged from the original simulations. Consequently, adjusted datasets do not reflect the brightening associated with aerosol reductions. Users should therefore exercise caution when employing adjusted data for applications directly dependent on radiative fluxes, such as solar energy assessments or photosynthesis modeling, as surface shortwave radiation will not be consistent with the adjusted temperature trajectory.



135



Despite these limitations, the method provides a practical framework for aligning existing high-resolution regional projections with updated warming constraints, for example for impact assessments focused on projected hydroclimatic changes.

# 2.3 Validation and truncation

To evaluate the quality of the adjustment, we compute an 'evolution score', a penalty-based diagnostic that quantifies how well the adjusted time series tracks the reference warming trajectory. The evolution score is calculated in moving windows and combines two components: deviations in slope and deviations in distance between the adjusted and reference series. If the score exceeds a threshold, the adjusted time series is truncated at that point, ensuring only the portion consistent with the reference trajectory is retained. This approach is similar in spirit to evaluation frameworks for scenario consistency (Tebaldi and Knutti, 2018).

Formally, we define a penalty score  $P_i$  for the i-th window that accounts for differences in both slope and magnitude. The metric is designed to be generous when the adjusted and reference series are approximately parallel, but penalizes substantial deviations in either slope or magnitude. The slope component  $C_s$  measures the normalized absolute difference in slopes:

Slope component 
$$C_s = \min\left(\frac{\left|s_i^{\text{adj}} - s_i^{\text{ref}}\right|}{0.15}, 1\right),$$
 (1)

where  $s_i^{\text{adj}}$  and  $s_i^{\text{ref}}$  denote the slopes of the adjusted and reference series in the *i*-th window. The distance component  $C_d$  represents the normalized mean absolute difference:

Distance component 
$$C_d = \min\left(\frac{\operatorname{mean}\left(|y_i^{\operatorname{adj}} - y_i^{\operatorname{ref}}|\right)}{0.3}, 1\right),$$
 (2)

where  $y_i^{\text{adj}}$  and  $y_i^{\text{ref}}$  are the corresponding temperature values. Both components are capped at 1 to prevent extreme differences from disproportionately influencing the score, ensuring the penalty remains bounded and interpretable. The overall penalty score combines both components with equal weighting:

Penalty score 
$$P_i = 0.5 C_s + 0.5 C_d$$
. (3)

Windows with  $P_i > 0.5$  are flagged as exhibiting significant divergence, triggering truncation at that point. The normalization factors (0.15 for slope, 0.3 for distance) and the overall evolution score threshold (0.5) were chosen empirically to balance strictness and flexibility in assessing trajectory consistency. These parameters can be adjusted depending on the specific application and desired level of conformity to the reference trajectory.

# 2.4 Sequential mapping to adjust global and regional warming

The method described above constitutes the base framework to establish regional warming consistency between CORDEX 0 RCM and CMIP6 GCM simulations, with results showcased in Fig. 2. We extend this approach by performing a two-step





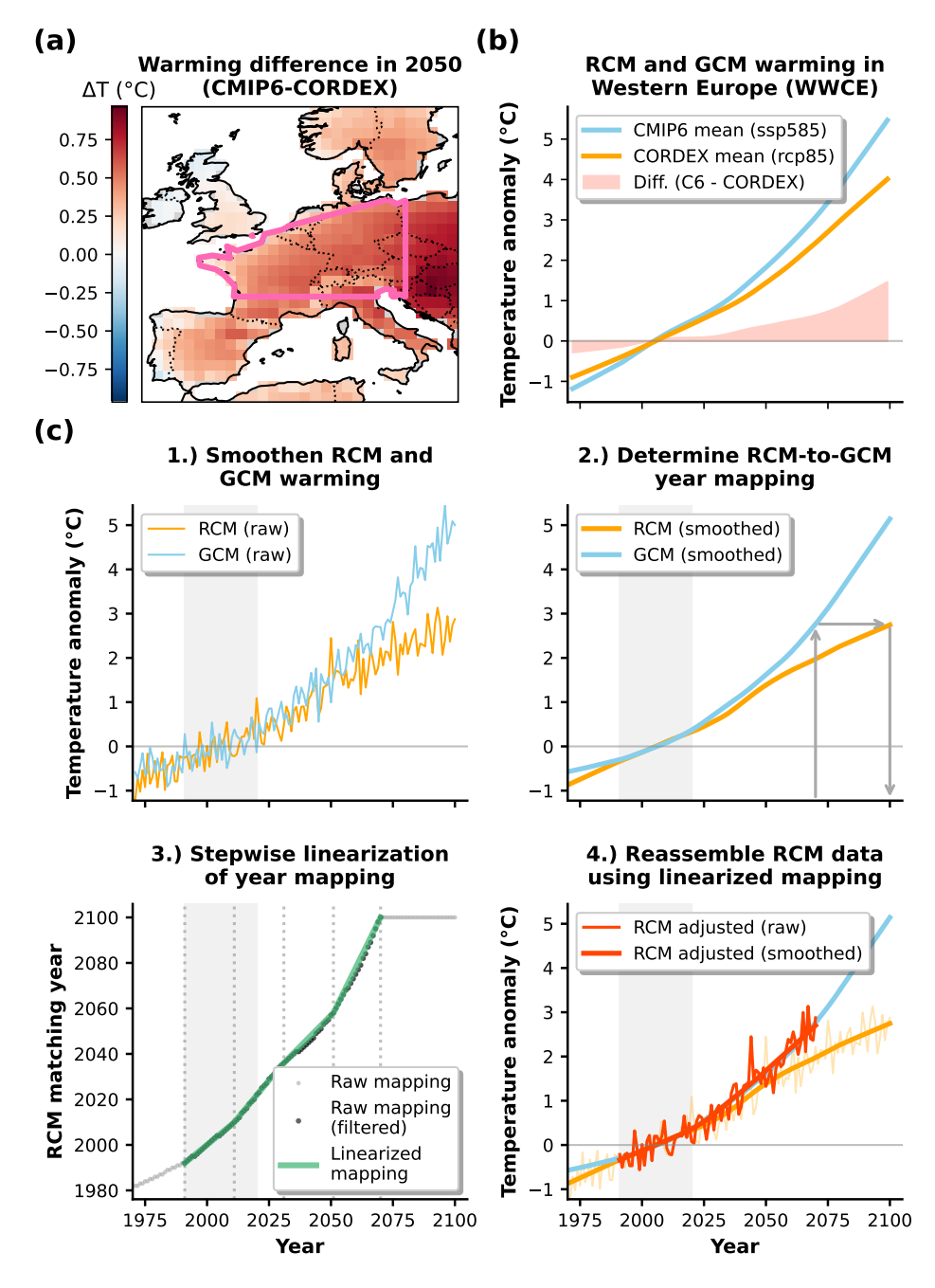


Figure 1. Overview of the warming adjustment for CORDEX RCM simulations. (a) Mean warming difference between the CMIP6 GCM ensemble and CMIP5-driven CORDEX simulations at mid-century (2050) under high-emission scenarios (SSP5-8.5 for CMIP6, RCP8.5 for CORDEX). Warming is computed from LOWESS-smoothed annual temperatures (up to 42 years) in 2050 relative to the 1991–2020 WMO reference period. (b) As in (a) but aggregated over Western Europe (pink contour) and shown as a time series. (c) Warming adjustment for a single RCM–GCM pair: (1) smoothing of RCM and GCM temperature time series via locally weighted regression; (2) temperature matching to define an initial year-to-year mapping; (3) linearization in 20-year segments with edge repeats filtered (grey markers); (4) reassembly of RCM data following the adjusted mapping.





sequential adjustment: first, the CMIP6 ensemble is adjusted to match prescribed global mean temperature (GMT) trajectories — specifically, the IPCC best estimate and 95th percentile warming projections (Lee et al., 2021) — using global-scale warming as the matching criterion (step 1 in Fig. 3a, outcome shown in Fig. 3b). Importantly, this adjustment is determined from the ensemble mean and then applied across the entire ensemble, preserving the model spread in terms of the timing at which individual simulations reach specific global warming levels, while ensuring that the ensemble mean aligns with the IPCC trajectories. Second, this global adjustment derived from the ensemble mean is then applied to individual CMIP6 models to modify their regional WWCE warming patterns accordingly (step 2 in Fig. 3a). Finally, we use this regionally adjusted CMIP6 WWCE warming (Fig. 3c) as the reference to adjust CORDEX simulations (step 3 in Fig. 3a). This sequential procedure establishes full consistency from the global to grid-cell scale: prescribed global warming targets, CMIP6 regional responses consistent with those global targets, and high-resolution CORDEX projections consistent with both.

Specifically, the adjustment proceeds as follows: the CMIP6 ensemble mean is first adjusted globally to match the IPCC GMT trajectories, yielding a single GCM-to-IPCC year mapping for a given emission scenario (e.g., SSP5-8.5; see Fig. 3b). This ensemble-wide mean mapping is then applied to individual CMIP6 models to derive adjusted warming patterns for WWCE, preserving each model's unique regional response chatateristics while ensuring consistency with the IPCC global warming trajectoeies. The resulting adjusted CMIP6 models are then used to derive the adjusted regional warming for WWCE. Finally, this adjusted WWCE warming from CMIP6 serves as the reference trajectory for adjusting CORDEX simulations (Fig. 3c). In doing so, we ensure that regional warming trajectories are consistent with prescribed global warming levels, aligning the methodology with recent GWL-based assessment frameworks (Schleussner et al., 2016; Seneviratne and Hauser, 2020).

# 3 Results and discussion

170

# 3.1 Demonstration of regional warming adjustment effects

To demonstrate the base framework, we first apply the direct GCM-RCM warming adjustment (without the IPCC global constraint) to CORDEX RCP8.5 simulations, examining the effects on temperature and precipitation projections throughout the 21st century. Applying the warming-adjustment algorithm to CORDEX RCP8.5 simulations reveals systematic modifications to both temperature and precipitation projections throughout the 21st century. Warming adjustment strengthens projected warming across Western Europe, with local differences exceeding 0.5°C by 2050 and a subtle east—west gradient (Fig. 2a). The stronger warming adjustment further east within and near our WWCE domain could be related to a weaker maritime influence as compared to more western areas. For spatial WWCE averages (Fig. 2b), adjusted warming deviates most notably before 2050 with regards to original simulations, after which differences remain approximately constant. For the low-emission RCP2.6 scenario, adjustments are comparatively minimal across the entire century. Overall, however, CMIP6-adjusted CORDEX RCM data feature comparable or stronger warming as a function of time.

For summer precipitation, the impact of warming adjustment is more complex, with regional contrasts emerging — adjusted data show enhanced wetting in the Northeast and stronger drying in the Southwest (Fig. 2c). These spatial patterns align



185

190

205

210

215



with projected large-scale changes under stronger warming: reduced summer rainfall in Mediterranean regions and increased precipitation at higher latitudes (Lee et al., 2021). Since CMIP6 models simulate stronger Western European warming than CMIP5-driven CORDEX simulations, the adjustment amplifies the north-south precipitation gradient consistent with this enhanced warming.

Examining WWCE spatial averages (Fig. 2d), we note that domain-wide aggregation masks some regional contrasts due to cancellation effects between wetting and drying areas. Nevertheless, the overall direction of projected precipitation changes remains consistent with original simulations, but with amplified magnitude. Under RCP2.6, adjusted precipitation increases more than in the original data, while under RCP8.5, it decreases more strongly, dominated by the southern drying signal. The RCP4.5 scenario shows intermediate behavior, with temporal variability reflecting the transition between low and high emission pathways.

These modifications demonstrate that warming adjustment not only accelerates projected temperature increases but also substantially alters precipitation trends in regionally complex ways. Although absolute differences are generally small, they represent additional shifts superimposed on the broader climate signals already present in original simulations. Even adjustments of a few percent in regional precipitation or fractions of a degree in temperature can amplify or dampen regional climate signals in ways that become important for impact assessments, particularly in domains such as water availability or heat stress, where sensitivity to relatively small changes is high.

## 200 3.2 Establishing consistent global-to-regional warming trajectories

To translate IPCC global warming trajectories into consistent regional high-resolution climate projections, we extend the base framework by performing a sequential two-step adjustment (Fig. 3a, detailed in Methods). First, CMIP6 models are adjusted to match prescribed IPCC global mean temperature trajectories—specifically, the best estimate and 95th percentile warming projections. Second, these globally adjusted CMIP6 models then serve as references for adjusting CORDEX RCM simulations. This procedure establishes full consistency across spatial scales: from global IPCC warming targets through CMIP6 regional responses to high-resolution CORDEX projections.

The CMIP6 ensemble employed here exhibits stronger global warming than the IPCC best estimate, though it remains well within the assessed 5th to 95th percentile range (Fig. 3b). Consequently, when CMIP6 models are adjusted to match the IPCC best estimate, their warming is reduced, while adjustment to the 95th percentile increases their warming trajectory. These global-scale adjustments propagate to the regional scale: adjusted WWCE warming is correspondingly lower or higher than in the original CMIP6 simulations depending on whether the best estimate or 95th percentile trajectory is targeted (Fig. 3c).

Both the IPCC best estimate and 95th percentile represent plausible futures within the evaluated uncertainty range rather than mutually exclusive outcomes. The best estimate offers a central projection for impact evaluation, while the 95th percentile highlights the potential for stronger, more widespread changes. Although differences in global mean warming between these pathways may appear modest, their implications at regional and sectoral scales can be disproportionately large. Small differences in global temperature trajectories translate into substantial variations in local weather and climate extremes, and impacts on climate-sensitive systems such as water resources, agriculture, and ecosystems.





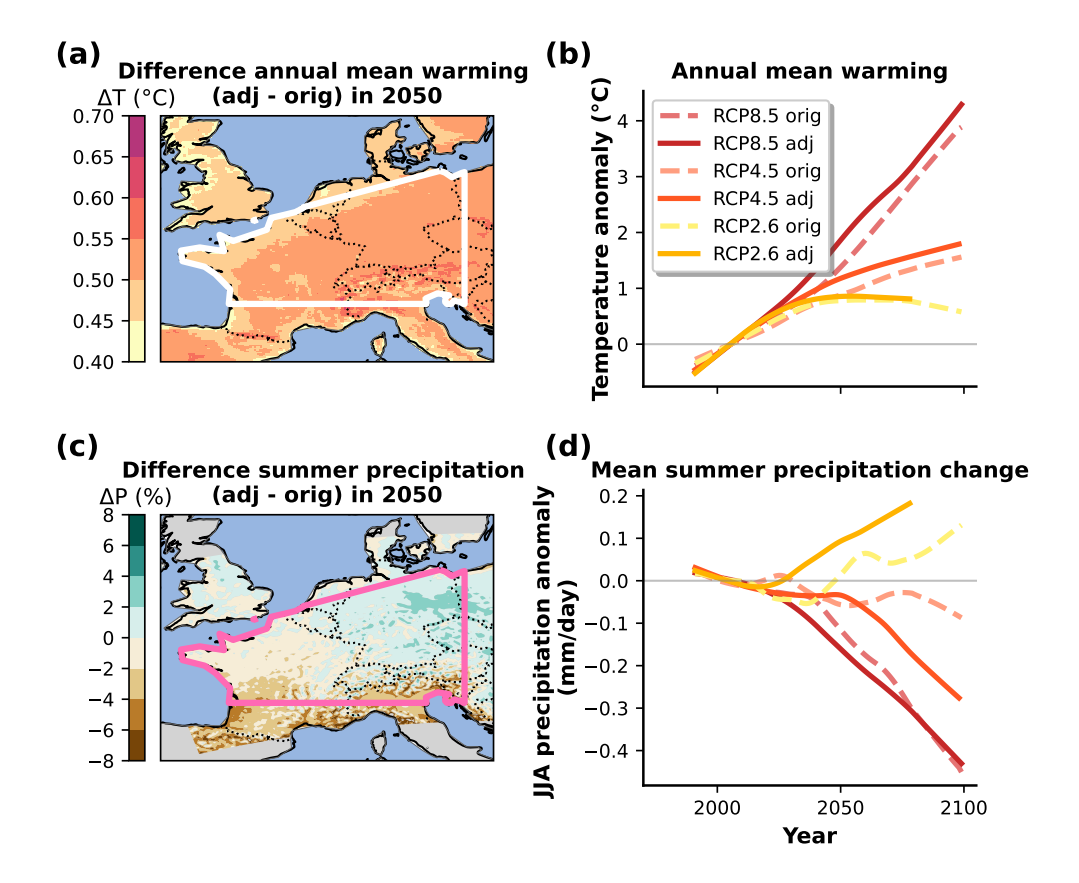


Figure 2. Effect of adjusting CORDEX RCM experiments to the Western European warming simulated by CMIP6 models. (a) Difference in annual mean warming between the adjusted and the original CORDEX temperature ensemble at mid-century (2050) under high-emission scenario RCP8.5. Warming is obtained by comparing LOWESS-smoothed annual temperatures (over at most 42 years) in 2050 to the current 1991-2020 WMO reference period. (b) Time series of annual mean warming (like (a)) of warming-adjusted (dashed) and original (solid) CORDEX temperature under low (RCP2.6), middle (RCP4.5) and high (RCP8.5) emission scenario, spatially aggregated over Western Europe. (c) Like (a) but displaying summer precipitation. (d) Like (b) but displaying mean summer precipitation change.

# 3.3 Effect of global-to-regional warming adjustment on high temperature and heavy precipitation extremes

Having established regionally consistent warming trajectories aligned with IPCC global targets, we now examine how these adjustments affect temperature and precipitation extremes, which are particularly relevant for impact assessments. Figure 4 illustrates the sensitivity of future extreme event magnitude changes to the choice between IPCC best estimate and 95th percentile warming trajectories.

For peak temperatures (TXx), differences between the two adjustment pathways are substantial and spatially coherent.

The 95th percentile adjustment consistently yields higher peak temperatures than the best estimate adjustment, with local

differences exceeding 0.6°C by 2050 (Fig. 4a). These spatial differences translate into systematic temporal evolution: across





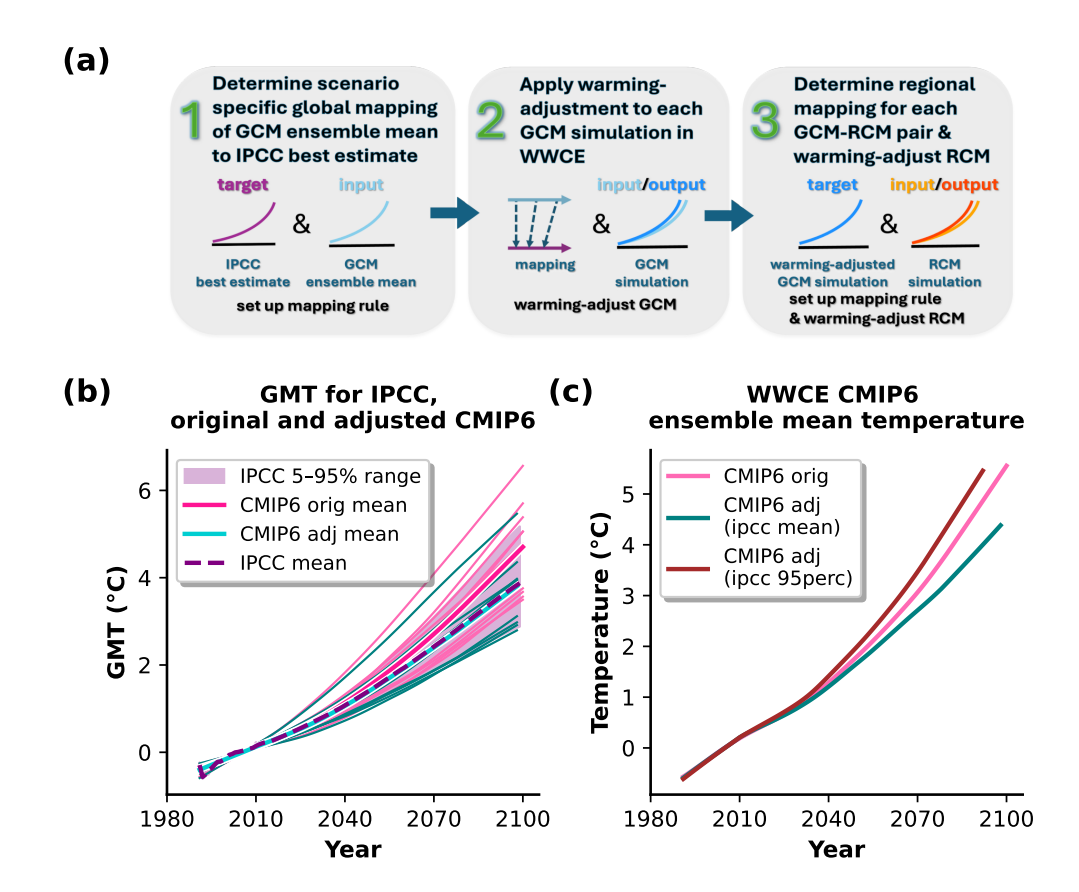


Figure 3. Overview of the warming adjustment to specific global target warming. a. Step-by-step visualization of the process with warming-adjustement of GCM and of RCM. b. Illustrating the global warming-adjustment of CMIP6 to IPCC mean for the high-emission scenario SSP5-8.5. The mean of the CMIP6 ensemble (pink) is adjusted to the IPCC target tragectory (purple dashed) and results in the adjusted CMIP6 ensemble mean (teal). The individual simulations of the ensemble are displayed as thin lines and adjusted according to the mapping, determined by the mean-adjustment. c. Illustrating the time series of the ensemble mean in WWCE for original CMIP6 ensemble (pink), the CMIP6 ensemble adjusted to IPCC mean (teal) and the CMIP6 ensemble adjusted to IPCC 95th percentile (brown).

the WWCE region, peak temperatures show progressive increases from original CORDEX through best estimate-adjusted to 95th percentile-adjusted datasets, with the latter consistently representing the highest values in both 2040 and 2060 (Fig. 4b). This demonstrates how the choice of global warming trajectory directly modulates not only regional mean temperature but also the magnitude of peak temperature events.

Precipitation extremes exhibit similar sensitivity to the adjustment pathway, though with more spatially complex patterns. Maximum 3-hour precipitation (Rx3hr) shows modest differences between the two adjustments—a few percent—with slightly enhanced precipitation in the northeast and reduced values in the southeast (Fig. 4c). Despite these small absolute differences,





temporal evolution reveals a consistent pattern: 95th percentile-adjusted data show progressively stronger increases in extreme precipitation compared to best estimate-adjusted data across both time periods examined (Fig. 4d).

These results demonstrate that warming adjustments consistent with IPCC global trajectories significantly influence both the magnitude and spatial patterns of regional extremes. The systematic amplification from best estimate to 95th percentile adjustments underscores the importance of considering multiple warming pathways when evaluating climate risks, particularly for extreme events with direct societal and ecological consequences.

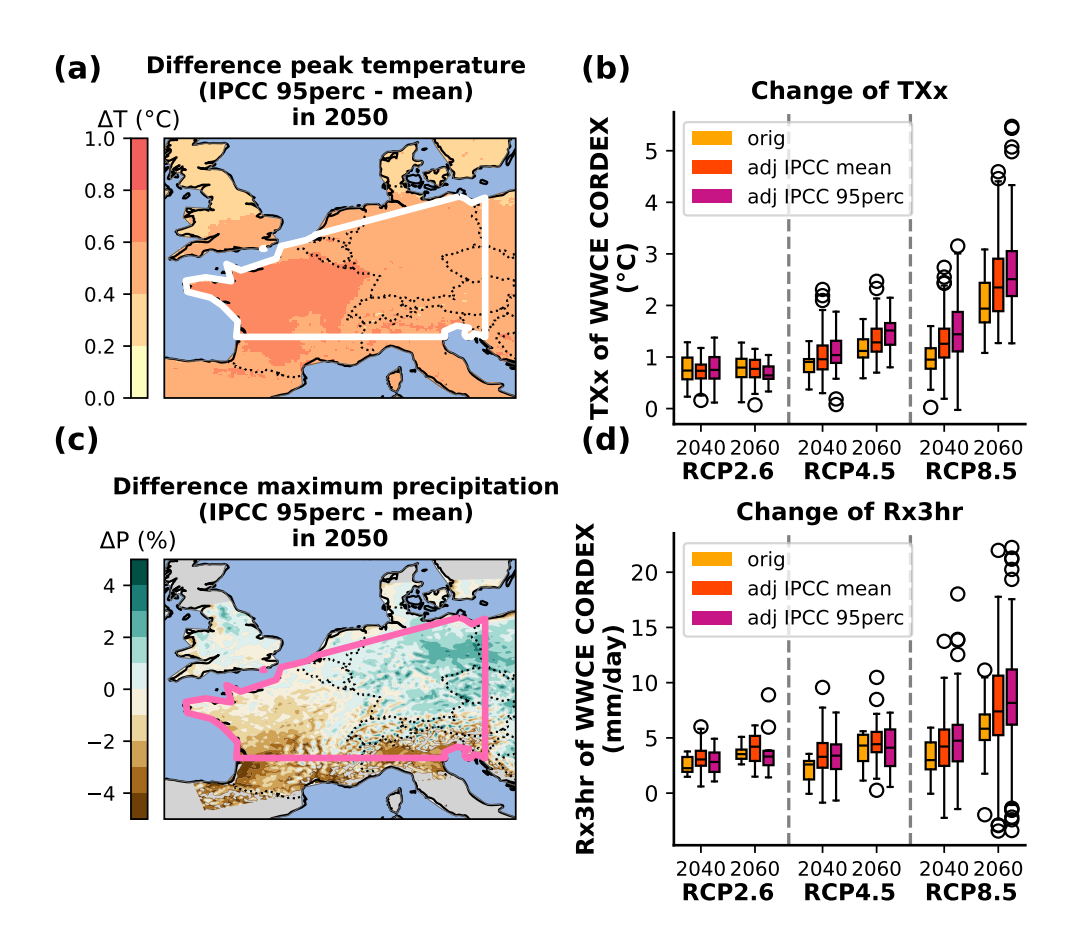


Figure 4. Projected future temperature and precipitation changes in warming-adjusted CORDEX RCM simulations consistent with IPCC global warming trajectories and CMIP6 models' regional warming responsedatasets. (a) Difference of the annual peak temperature between adjusted CORDEX temperature ensembles, once being adjusted to IPCC mean and once to IPCC 95th percentile, at mid-century (2050) under high-emission scenario RCP8.5. The peak temperature is obtained by comparing LOWESS-smoothed annual peak temperatures temperatures (over at most 42 years) in 2050 to the current 1991-2020 WMO reference period. (b) Change in peak temperature calculated like (a), but displaying change peak temperatures of original (yellow), IPCC mean adjusted (red) and IPCC 95th percentile (purple) adjusted peak temperatures, spatially aggregated over Western Europe (white contour line in (a)), in 2040 and 2060. (c) Like (a), but difference in maximum precipitation. (d) Like (b), but change in maximum precipitation.





# 3.4 Implications for climate impact assessments

Our analyses demonstrate that warming adjustment systematically modifies projected climate trajectories while preserving physical consistency across spatial scales. The CMIP6-only adjustment consistently amplifies warming pace relative to original CMIP5-CORDEX simulations, with largest differences emerging in the first half of the 21st century. For precipitation, adjustments lead to regionally distinct modifications, producing shifts in wetting and drying patterns that can diverge substantially from unadjusted projections. These outcomes reflect an additional information layer rather than statistical artifacts, providing complementary perspectives to original CMIP6 simulations by highlighting potential sensitivities and uncertainties in future climate projections. These findings underscore the importance of considering both best estimate and upper-range trajectories when assessing climate impacts. This approach enables comprehensive evaluation of possible futures and provides critical insights into robustness and variability of projected outcomes. Such broader perspective is essential for informing adaptation planning and mitigation strategies, ensuring decision-making accounts for not only central tendencies but also upper-end risks that, while less likely, may carry the most severe consequences for ecosystems, water resources, agriculture, and human health (Bezner Kerr et al., 2022; Rogelj et al., 2019).

#### 4 Conclusions

255

260

265

The warming adjustment presented here provides a practical framework for aligning existing high-resolution regional climate model simulations with the latest generation of global models and scenarios. Importantly, these datasets are not intended to replace CMIP6-CORDEX simulations, but rather to bridge the temporal gap until next-generation regional downscaling experiments become available. The approach establishes consistency from global IPCC warming targets through CMIP6 regional responses to high-resolution CORDEX projections, enabling seamless translation of large-scale climate signals into regional contexts while preserving fine-scale spatial detail.

A key advantage of this framework is its flexibility. The method can be applied to different regions, variables, emission scenarios, and temporal resolutions, allowing researchers to tailor analyses to specific scientific or policy-relevant questions. By providing adjusted datasets consistent with CMIP6 regional patterns, the approach enhances the interpretability and utility of regional projections for impact assessments, adaptation planning, and policy development.

Several methodological considerations warrant attention. As detailed in Section 2.5, the adjustment is most appropriate for temperature-driven climate variables. Users should exercise caution when applying adjusted data to variables with temporal memory effects (e.g., soil moisture) or those directly dependent on radiative fluxes (e.g., surface shortwave radiation), as the reassembly of existing simulation years does not modify the underlying radiation fields. Despite these limitations, the framework offers a scientifically rigorous approach to harmonizing regional projections with updated global constraints.

Given that CMIP6-CORDEX simulations remain under development while CMIP7 is already on the horizon, this warming adjustment framework provides a timely solution for bridging generational gaps in climate projections. The methodology is openly available, and we encourage the research community to apply and extend this approach for regional climate assessments





worldwide. Ultimately, this work facilitates more consistent interpretation of climate information across spatial scales and supports better-informed decision-making for climate adaptation and mitigation strategies.

Code and data availability. A demonstration version of the code to understand the method in this study is publicly available at https://doi.org/10.5281/zenodo.17289501 under an MIT license. The demo includes sample data generation and the warming adjustment itself, illustrating key processing steps.

# Appendix A

275

280

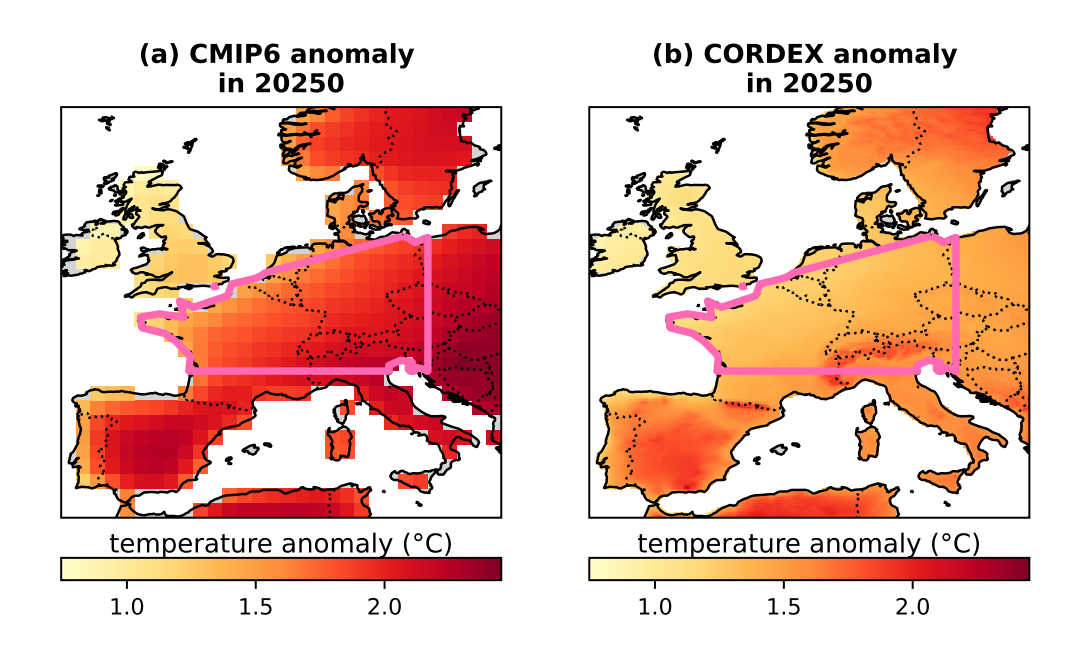
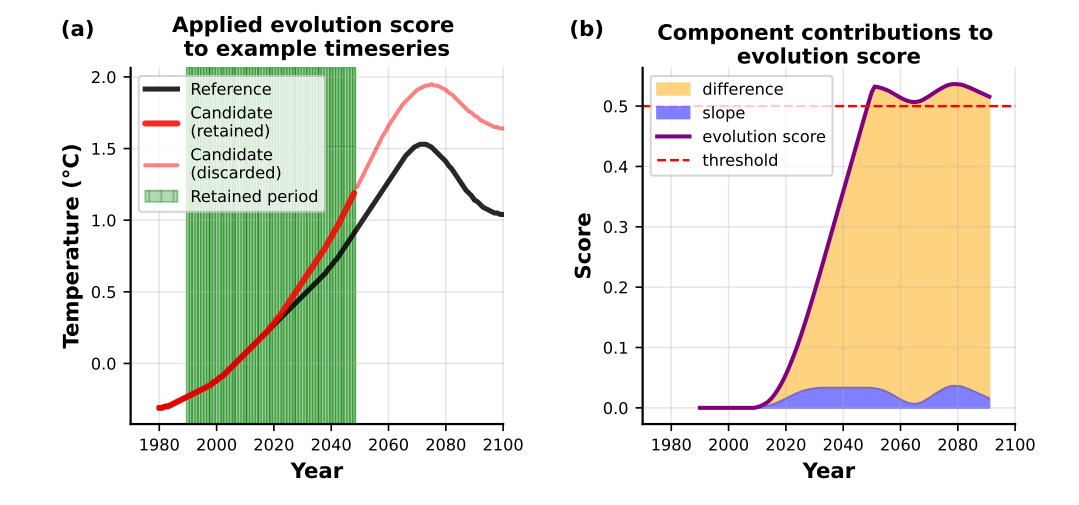


Figure A1. Overview of the warming for CMIP6 GCM and CORDEX RCM simulations. (a) Mean warming of CMIP6 global climate model ensemble at mid-century (2050) under high-emission scenarios (SSP5-8.5). Warming is obtained like Fig. 1a. (b) Like (a), but for current CMIP5-driven CORDEX simulations unter RCP8.5.

Author contributions. S.B. led the conceptualization, analysis, and writing of the manuscript. D.L.S. contributed substantially to the development of the methodology, data analysis, and interpretation of results, and provided critical input throughout the writing process. S.I.S. conceived the study, provided conceptual guidance, and supervision. All authors discussed the results and approved the final version of the paper.







**Figure A2. Evolution score illustrated with an example.** (a) Example time series are used as candidate and reference and the retained period, resulting from the evolution score and dependent on the threshold, is highlighted. (b) Evolution score of the candidate time series for each point in time (purple) and broken down into the contributions of its individual components (difference component in yellow and slope component in blue). The threshold (red dashed, 0.5) marks where the time series retained or discarded part. When the threshold is reached, the time series is cut off.

*Competing interests.* Sonia I. Seneviratne is a member of the editorial board of Earth System Dynamics. The authors declare that they have no other competing interests.

Acknowledgements. S.B. acknowledges funding from the Joint Initiative SPEED2ZERO and D.L.S. acknowledges partial funding from the European Union's Horizon 2020 research and innovation program for the XAIDA project under Grant Agreement 101003469.

285 We also thank Mathias Hauser for his critical input and support in data processing.





#### References

290

295

300

- Bartók, B., Wild, M., Folini, D., Lüthi, D., Kotlarski, S., and Schär, C.: Projected changes in surface solar radiation in CMIP5 global climate models and in EURO-CORDEX regional climate models for Europe, Clim. Dyn., 49, 2665–2683, https://doi.org/10.1007/s00382-016-3471-2, 2017.
- Bezner Kerr, R., Hasegawa, T., Lasco, R., Bhatt, I., Deryng, D., Farrell, A., Gurney-Smith, H., Ju, H., Lluch-Cota, S., Meza, F., Nelson, G., Neufeldt, H. and, ., and Thornton, P.: Food, Fibre, and Other Ecosystem Products, in: Climate Change 2022: Impacts, Adaptation and Vulnerability. Contribution of Working Group II to the Sixth Assessment Report of the Intergovernmental Panel on Climate Change, edited by Pörtner, H. O., Roberts, D. C., Tignor, M., Poloczanska, E. S., Mintenbeck, K., Alegría, A., Craig, M., Langsdorf, S., Löschke, S., Möller, V., Okem, A., and Rama, B., book section 5, Cambridge University Press, Cambridge, UK and New York, NY, USA, https://doi.org/10.1017/9781009325844.007, 2022.
- Boé, J., Somot, S., Corre, L., and Nabat, P.: Large discrepancies in summer climate change over Europe as projected by global and regional climate models: causes and consequences, Clim. Dyn., 54, 2981–3002, https://doi.org/10.1007/s00382-020-05153-1, 2020.
- Diez-Sierra, J., Iturbide, M., Fernández, J., Gutiérrez, J., Milovac, J., and Cofiño, A.: Consistency of the regional response to global warming levels from CMIP5 and CORDEX projections, Climate Dynamics, https://doi.org/10.1007/s00382-023-06790-y, 2023.
- Eyring, V., Bony, S., Meehl, G. A., Senior, C. A., Stevens, B., Stouffer, R. J., and Taylor, K. E.: Overview of the Coupled Model Intercomparison Project Phase 6 (CMIP6) experimental design and organization, Geoscientific Model Development, 9, 1937–1958, https://doi.org/10.5194/gmd-9-1937-2016, 2016.
- Giorgi, F. and Gutowski Jr., W. J.: Regional Dynamical Downscaling and the CORDEX Initiative, Annual Review of Environment and Resources, 40, 467–490, https://doi.org/10.1146/annurev-environ-102014-021217, 2015.
  - Gutowski Jr., W. J., Giorgi, F., Timbal, B., Frigon, A., Jacob, D., Kang, H.-S., Raghavan, K., Lee, B., Lennard, C., Nikulin, G., O'Rourke, E., Rixen, M., Solman, S., Stephenson, T., and Tangang, F.: WCRP COordinated Regional Downscaling Experiment (CORDEX): a diagnostic MIP for CMIP6, Geoscientific Model Development, 9, 4087–4095, https://doi.org/10.5194/gmd-9-4087-2016, 2016.
- Iturbide, M., Gutiérrez, J. M., Alves, L. M., Bedia, J., Cerezo-Mota, R., Cimadevilla, E., Cofiño, A. S., Di Luca, A., Faria, S. H., Gorodet-skaya, I. V., Hauser, M., Herrera, S., Hennessy, K., Hewitt, H. T., Jones, R. G., Krakovska, S., Manzanas, R., Martínez-Castro, D., Narisma, G. T., Nurhati, I. S., Pinto, I., Seneviratne, S. I., van den Hurk, B., and Vera, C. S.: An update of IPCC climate reference regions for subcontinental analysis of climate model data: definition and aggregated datasets, Earth System Science Data, 12, 2959–2970, https://doi.org/10.5194/essd-12-2959-2020, 2020.
- Jacob, D., Petersen, J., Eggert, B., Alias, A., Christensen, O. B., Bouwer, L. M., Braun, A., Colette, A., Déqué, M., Georgievski, G., Georgopoulou, E., Gobiet, A., Menut, L., Nikulin, G., Haensler, A., Hempelmann, N., Jones, C., Keuler, K., Kovats, S., Kröner, N., Krüger, O., Lenderink, G., Ludwig, R., Mares, C., van Meijgaard, E., Moseley, C., Pfeifer, S., Preuschmann, S., Radermacher, C., Radtke, K., Rechid, D., Rounsevell, M., Samuelsson, P., Somot, S., Soussana, J.-F., Teichmann, C., Valentini, R., Vautard, R., Weber, B., and Yiou, P.: EURO-CORDEX: new high-resolution climate change projections for European impact research, Reg. Environ. Change, 14, 563–578, https://doi.org/10.1007/s10113-013-0499-2, 2014.
- Lee, J.-Y., Marotzke, J., Bala, G., Cao, L., Corti, S., Dunne, J., Engelbrecht, F., Fischer, E., Fyfe, J., Jones, C., Maycock, A., Mutemi, J., Ndiaye, O., Panickal, S., and Zhou, T.: Future Global Climate: Scenario-Based Projections and Near-Term Information Supplementary Material, in: Climate Change 2021: The Physical Science Basis. Contribution of Working Group I to the Sixth Assessment Report of the Intergovernmental Panel on Climate Change, edited by Masson-Delmotte, V., Zhai, P., Pirani, A., Connors, S. L., Péan, C., Berger, S.,



345



- Caud, N., Chen, Y., Goldfarb, L., Gomis, M. I., Huang, M., Leitzell, K., Lonnoy, E., Matthews, J. B. R., Maycock, T. K., Waterfield, T.,

  Yelekçi, O., Yu, R., and Zhou, B., book section 4, pp. 1–108, Cambridge University Press, Cambridge, UK and New York, NY, USA,

  https://www.ipcc.ch/report/ar6/wg1/downloads/report/IPCC\_AR6\_WGI\_Chapter04\_SM.pdf, 2021.
  - Li, C., Zwiers, F., Zhang, X., Li, G., Sun, Y., and Wehner, M.: Changes in Annual Extremes of Daily Temperature and Precipitation in CMIP6 Models, Journal of Climate, 34, 3441 3460, https://doi.org/10.1175/JCLI-D-19-1013.1, 2021.
- Meehl, G. A., Senior, C. A., Eyring, V., Flato, G., Lamarque, J.-F., Stouffer, R. J., Taylor, K. E., and Schlund, M.: Context for interpreting equilibrium climate sensitivity and transient climate response from the CMIP6 Earth system models, Science Advances, 6, eaba1981, https://doi.org/10.1126/sciadv.aba1981, 2020.
  - Persad, G., Samset, B. H., Wilcox, L. J., Allen, R. J., Bollasina, M. A., Booth, B. B. B., Bonfils, C., Crocker, T., Joshi, M., and Lund, M. T.: Rapidly evolving aerosol emissions are a dangerous omission from near-term climate risk assessments, Environ. Res.: Climate, 2, 032 001, https://doi.org/10.1088/2752-5295/acd6af, 2023.
- Rogelj, J., Forster, P. M., Kriegler, E., Smith, C. J., Clarke, L., Geden, O., Krey, V., Luderer, G., Riahi, K., Schaeffer, M., Vuuren, D. P. v., and Yeo, S.: Estimating and tracking the remaining carbon budget for stringent climate targets, Nature, 571, 335–342, https://doi.org/10.1038/s41586-019-1368-z, 2019.
  - Scherrer, S. C., de Valk, C., Begert, M., Gubler, S., Kotlarski, S., and Croci-Maspoli, M.: Estimating trends and the current climate mean in a changing climate, Climate Services, 33, 100 428, https://doi.org/https://doi.org/10.1016/j.cliser.2023.100428, 2024.
- Schleussner, C.-F., Lissner, T. K., Fischer, E. M., Wohland, J., Perrette, M., Golly, A., Rogelj, J., Childers, K., Schewe, J., Frieler, K., Mengel, M., Hare, W., and Schaeffer, M.: Differential climate impacts for policy-relevant limits to global warming: the case of 1.5 °C and 2 °C, Earth System Dynamics, 7, 327–351, https://doi.org/10.5194/esd-7-327-2016, 2016.
  - Schumacher, D. L., Singh, J., Hauser, M., Persad, G., Wild, M., Boé, J., and Seneviratne, S. I.: Exacerbated summer European warming not captured by climate models neglecting long-term aerosol changes, Commun. Earth Environ., 5, 182, https://doi.org/10.1038/s43247-024-01332-8, 2024.
  - Seneviratne, S., Zhang, X., Adnan, M., Badi, W., Dereczynski, C., Di Luca, A., Ghosh, S., Iskandar, I., Kossin, J., Lewis, S., Otto, F., Pinto, I., Satoh, M., Vicente-Serrano, S., Wehner, M., and Zhou, B.: Weather and Climate Extreme Events in a Changing Climate, in: Climate Change 2021: The Physical Science Basis. Contribution of Working Group I to the Sixth Assessment Report of the Intergovernmental Panel on Climate Change, edited by Masson-Delmotte, V., Zhai, P., Pirani, A., Connors, S. L., Péan, C., Berger, S., Caud, N.,
- Chen, Y., Goldfarb, L., Gomis, M. I., Huang, M., Leitzell, K., Lonnoy, E., Matthews, J. B. R., Maycock, T. K., Waterfield, T., Yelekçi, O., Yu, R., and Zhou, B., book section 11, pp. 1513–1765, Cambridge University Press, Cambridge, UK and New York, NY, USA, https://doi.org/10.1017/9781009157896.013, 2021.
  - Seneviratne, S. I. and Hauser, M.: Regional Climate Sensitivity of Climate Extremes in CMIP6 Versus CMIP5 Multimodel Ensembles, Earth's Future, 8, e2019EF001474, https://doi.org/https://doi.org/10.1029/2019EF001474, e2019EF001474 2019EF001474, 2020.
- Sobolowski, S., Somot, S., Fernandez, J., Evin, G., Maraun, D., Kotlarski, S., Jury, M., Benestad, R. E., Teichmann, C., Christensen, O. B., Katharina, B., Buonomo, E., Katragkou, E., Steger, C., Sørland, S., Nikulin, G., McSweeney, C., Dobler, A., Palmer, T., Wilke, R., Boé, J., Brunner, L., Ribes, A., Qasmi, S., Nabat, P., Sevault, F., Oudar, T., and Brands, S.: EURO-CORDEX GCM Selection & Ensemble Design: Implementation Framework, https://doi.org/10.5281/zenodo.7673400, 2023.
- Tebaldi, C. and Knutti, R.: Evaluating the accuracy of climate change pattern emulation for low warming targets, Environmental Research

  Letters, 13, 055 006, https://doi.org/10.1088/1748-9326/aabef2, 2018.



370



- Tebaldi, C., Snyder, A., and Dorheim, K.: STITCHES: creating new scenarios of climate model output by stitching together pieces of existing simulations, Earth System Dynamics, 13, 1557–1609, https://doi.org/10.5194/esd-13-1557-2022, 2022.
- Tokarska, K. B., Stolpe, M. B., Sippel, S., Fischer, E. M., Smith, C. J., Lehner, F., and Knutti, R.: Past warming trend constrains future warming in CMIP6 models, Science Advances, 6, eaaz9549, https://doi.org/10.1126/sciadv.aaz9549, 2020.
- Wehner, M. F.: Characterization of long period return values of extreme daily temperature and precipitation in the CMIP6 models: Part 2, projections of future change, Weather and Climate Extremes, 30, 100 284, https://doi.org/https://doi.org/10.1016/j.wace.2020.100284, 2020.
  - Wild, M., Gilgen, H., Roesch, A., Ohmura, A., Long, C. N., Dutton, E. G., Forgan, B., Kallis, A., Russak, V., and Tsvetkov, A.: From Dimming to Brightening: Decadal Changes in Solar Radiation at Earth's Surface, Science, 308, 847–850, https://doi.org/10.1126/science.1103215, 2005.
  - Wild, M., Wacker, S., Yang, S., and Sanchez-Lorenzo, A.: Evidence for Clear-Sky Dimming and Brightening in Central Europe, Geophysical Research Letters, 48, e2020GL092216, https://doi.org/https://doi.org/10.1029/2020GL092216, e2020GL092216 2020GL092216, 2021.
- Zelinka, M. D., Myers, T. A., McCoy, D. T., Po-Chedley, S., Caldwell, P. M., Ceppi, P., Klein, S. A., and Taylor, K. E.: Causes of Higher Climate Sensitivity in CMIP6 Models, Geophysical Research Letters, 47, e2019GL085782, https://doi.org/10.1029/2019GL085782, e2019GL085782 10.1029/2019GL085782, 2020.